Petroleum Analysis with a Softer Touch: Try GCxGC/FI

AccuTOF™ GC-Alpha

JEOL
Solutions for Innovation

Received: 29 September 2019 | Revised: 24 March 2020 | Accepted: 24 March 2020

DOI: 10.1002/rcm.8793

SPECIAL ISSUE PAPER

Rapid Communications in Mass Spectrometry WILEY

Comparison of gaseous ubiquitin ion structures obtained from a solid and solution matrix using ion mobility spectrometry/mass spectrometry

Ellen D. Inutan[1,2,3] | Dean R. Jarois[2] | Christopher B. Lietz[2] | Tarick J. El-Baba[4] | Efstathios A. Elia[2] | Santosh Karki[2] | Andjoe A.S. Sampat[2] | Casey D. Foley[2] | David E. Clemmer[4] | Sarah Trimpin[1,2]

[1]MSTM, LLC, Newark, DE, USA

[2]Department of Chemistry, Wayne State University, Detroit, MI, USA

[3]Mindanao State University–Iligan Institute of Technology, Iligan City, Philippines

[4]Department of Chemistry, Indiana University, Bloomington, IN, USA

Correspondence
E. D. Inutan, Mindanao State University–Iligan Institute of Technology, Iligan City, Philippines.
Email: ellen.inutan@g.msuiit.edu.ph

S. Trimpin, Department of Chemistry, Wayne State University Detroit, MI, USA.
Email: sarah.trimpin@wayne.edu

Funding information
NSF CHE, Grant/Award Number: (CMI)-1411376; NSF CAREER; Wayne State University

Rationale: Examining surface protein conformations, and especially achieving this with spatial resolution, is an important goal. The recently discovered ionization processes offer spatial-resolution measurements similar to matrix-assisted laser desorption/ionization (MALDI) and produce charge states similar to electrospray ionization (ESI) extending higher-mass protein applications directly from surfaces on high-performance mass spectrometers. Studying a well-interrogated protein by ion mobility spectrometry-mass spectrometry (IMS-MS) to access effects on structures using a solid *vs.* solvent matrix may provide insights.

Methods: Ubiquitin was studied by IMS-MS using new ionization processes with commercial and homebuilt ion sources and instruments (Waters SYNAPT G2(S)) and homebuilt 2 m drift-tube instrument; MS™ sources). Mass-to-charge and drift-time (t_d)-measurements are compared for ubiquitin ions obtained by *inlet* and *vacuum* ionization using laserspray ionization (LSI), matrix- (MAI) and solvent-assisted ionization (SAI), respectively, and compared with those from ESI under conditions that are most comparable.

Results: Using the same solution conditions with SYNAPT G2(S) instruments, t_d-distributions of various ubiquitin charge states from MAI, LSI, and SAI are similar to those from ESI using a variety of solvents, matrices, extraction voltages, a laser, and temperature only, showing subtle differences in more compact features within the elongated distribution of structures. However, on a homebuilt drift-tube instrument, within the elongated distribution of structures, both similar and different t_d-distributions are observed for ubiquitin ions obtained by MAI and ESI. MAI-generated ions are frequently narrower in their t_d-distributions.

Conclusions: Direct comparisons between ESI and the new ionization methods operational directly from surfaces suggest that the protein in its solution structure prior to exposure to the ionization event is either captured (frozen out) at the time of crystallization, or that the protein in the solid matrix is associated with sufficient solvent to maintain the solution structure, or, alternatively, that the observed structures are those related to what occurs in the gas phase with ESI- or MAI-generated ions and not with the solution structures.

1 | INTRODUCTION

Understanding molecular conformations and related folding processes is a key challenge in chemistry and biology. The toolbox for studying native structures within or directly from their natural environments such as (bio)films or tissues is limited and frequently only accessible indirectly. Over the past three decades, electrospray ionization (ESI) has evolved as the ionization method of choice for mass spectrometry (MS) studies related to ion structures because of its "softness".[1,2] In ESI, the molecule of interest is dissolved in a solvent, typically a buffer, and ion formation is initiated by the application of a high voltage to a capillary supplying the analyte solution. A number of variables can influence the gas-phase ESI ion structures including solution conditions, inlet temperature, ionizing and extraction voltages, as well as the ionization process itself.[3–9] The significance of successes in this area is reflected in the growing field of native MS.[10–15]

Direct analysis of the chemical composition of surfaces is available by various extraction protocols, most notably desorption ESI (DESI) and liquid junction approaches.[16–25] However, the ability to maintain solution-phase structures in the gas phase is still open to question, especially structural changes which occur upon loss of the final water molecules.[26] In the matrix-assisted ionization (MAI) method, the analyte is initially in solution similar to ESI or matrix-assisted laser desorption/ionization (MALDI), but ionization occurs from the solid state as in MALDI. However, unlike MALDI, the ions produced have charge states very similar to those from ESI allowing direct comparison of structures with ionization from a solid and solvent matrix. The outcome has the potential to address issues related to both the ionization process in MAI and how ionization from a solid matrix affects gas-phase structures.

The new ionization processes may also help address current surface analyses limitations using ion mobility spectrometry (IMS)-MS.[27–30] The ion abundances and charge states using these ionization processes are surprisingly similar to those obtained by ESI,[30,31] so that mechanistic commonalities might be expected.[32] A proposed mechanism is that bare gas-phase analyte ions are formed from highly charged matrix:analyte particles by a desolvation process leading to the removal of the solid or solution matrix, similar to ESI.[32] The charged particles are produced under conditions leading to matrix evaporation/sublimation without the requirement of voltage, laser ablation, or, for some matrices, even application of heat. Ions of fragile functionalities were measured intact using MAI initiated by a laser ablation event, referred to as laserspray ionization (LSI).[32,33] The laser functions to ablate matrix particles from a spatially resolved area.[33–36] Instead of a laser, a pellet gun was used to produce an acoustic (shock) wave to ablate matrix:analyte into the inlet, initiating ionization even of proteins directly from a surface, clearly demonstrating that the laser is not directly involved in the ionization event leading to multiply charged ions.[37] LSI imaging was accomplished with competitive spatial resolution and speed using transmission geometry laser alignment relative to the inlet/mass analyzer of the mass spectrometer.[38] Low spatial resolution analysis can be accomplished without a laser using MAI or solvent-assisted ionization (SAI) in which the matrix is the solvent.[31,39,40]

With these *inlet* and *vacuum* ionization methods, exposing the matrix:analyte sample to the pressure differential in the inlet has produced protein ions from species as large as bovine serum albumin.[27,31,41–43] Unlike SAI,[44,45] MAI also readily operates from direct introduction into intermediate pressure without use of an atmospheric pressure inlet.[31] Using solid matrices, matrix:analyte samples that are still 'wet' when introduced into the vacuum of the mass spectrometer have resulted in improved ion abundance, but also are more prone to carryover between samples.[46] Similarly, the addition of solid matrices to a large excess of solvent, a SAI sample, lowered the heat requirements of the inlet tube relative to more aqueous solutions,[47] and the addition of ammonium salts 'cleans up' mass spectra.[48]

Unfortunately, the most effective MAI matrices, e.g., 3-nitrobenzonitrile (3-NBN) and 1,2-dicyanobenzene, are the only ones soluble in high organic content solvents which are not compatible with native protein structures.[31,46,49] A few MAI matrices, such as 2-bromo-2-nitro-1,3-propanediol (bronopol) and 2-methyl-2-nitro-1,3-propanediol (MNP),[46] are soluble in aqueous solution, and increased water content in sample preparation requires added inlet heat for effective, spontaneous ionization, which is often not available with commercial inlets,[50,51] and consequently requires retrofits for improved performance.[30,52,53] Solvent conditions have been shown to affect both the conformations of ubiquitin observed by ESI-IMS-MS and the charge-state distributions. Here we assess whether the solution conditions are still important when a solid matrix is used in MAI, relative to a solution matrix in ESI, by making comparisons between IMS-MS using MAI with various solvent compositions including 100% water and ESI using the well-studied protein ubiquitin.[4–8,54–63]

2 | EXPERIMENTAL

2.1 | Materials

All chemicals and solvents were obtained from Sigma-Aldrich Inc. (St Louis, MO, USA), including the previously discovered matrices[31,46]: 3-NBN, MNP, 2-aminobenzoyl alcohol (2-ABA), 3,6-dibromocarbazole, 3-bromocarbazole, *N*-isopropyl-9*H*-carbazole, *N*-propyl-9*H*-carbazole, 2,5-dihydroxybenzoic acid (2,5-DHB), stearic acid and ubiquitin. 2,5-Dihydroxyacetophenone (2,5-DHAP, 97% purity), acetonitrile (ACN), ammonium hydroxide and formic acid (FA) were obtained from Fisher Scientific Inc. (Pittsburgh, PA, USA). HPLC grade methanol (MeOH) and water were purchased from EMD Chemicals (Gibbstown, NJ, USA) and acetic acid (AA) from Mallinckrodt Chemicals (Phillipsburg, NJ, USA). Plain microscopy glass slides used were made by Gold Seal Products (Portsmouth, NH, USA).

2.2 | Sample preparation

Stock solutions of 1 mg mL^{-1} were prepared in water. Approximately 5 mg of each matrix was used and individually prepared as a saturated solution as described previously.[46] For LSI using 2,5-DHAP in 150 μL 50:50 ACN/water (warmed), a layer method was used.[51,64] A volume of 1 μL of the analyte (e.g., 5 pmol) was placed on the glass plate and 1–2 μL of the matrix solution then added, mixed using the pipet tip and air dried. The vacuum LSI sample spot was a prepared, premixed matrix:analyte mixture (5 or 10 pmol analyte added with matrix solution in 1:1 volume ratio), and 1 μL was spotted on top of the target plate, preferably a glass microscope slide, using the dried-droplet method.[51] The final concentrations of the analytes on the glass plate ranged from 2.5 pmol to 5 pmol.

2.3 | IMS-MS conditions on commercial instruments

More extensive specific details on the inlet source conditions and modifications are given in the supporting information and include Figures S1 to S14 as well as Schemes S1 and S2. Previously described IMS-MS conditions were used.[50,64] Nitrogen gas was used for the drift-time (t_d) separation with a flow rate of 22 mL min^{-1} and the pressure in the drift cell was 3.19 mbar. The wave velocity used ranged from 450 to 652 m s^{-1} and the IMS wave height was set at 40 V unless otherwise noted.

2.4 | LSI on the SYNAPT G2

A nanoESI source was used on a SYNAPT G2 mass spectrometer[65] (Waters, Wilmslow, UK) to perform LSI. The LockSpray of the nanoESI source was removed and a fabricated desolvation device was used as previously described.[50] The laser was aligned in transmission geometry relative to the inlet/mass analyzer, as previously described.[34,50]

2.5 | MAI from atmospheric and intermediate pressure on the SYNAPT G2(S)

Waters SYNAPT G2(S) mass spectrometers equipped with a commercial intermediate pressure MALDI source were used to carry out *vacuum* MAI (*v*MAI). For *v*MAI using the intermediate pressure MALDI source without engaging the laser, acquisitions were performed in positive ion and sensitivity modes using the LSI settings as previously described.[31,46,47,49] Alternatively, a homebuilt *vacuum*-probe source was used for *v*MAI.[30,52] For MAI at atmospheric pressure, either the MS™ (Newark, DE USA) Ionique manual platform was used, or the (nano)ESI source was overridden using a source adapter plug (to provide open access to the skimmer cone) as previously described.[46,66]

2.6 | ESI on the SYNAPT G2(S)

Waters SYNAPT G2(S) mass spectrometers were used to perform ESI and nanoESI. Default settings were used: 40 V cone voltage, 3.4 kV spray voltage, and 80 °C source temperature. Alternatively, the same conditions may also be employed on the MS™ Ionique manual platform with the help of a retrofitted MS™ inlet tube.[40]

2.7 | SAI on the SYNAPT G2S

A Waters SYNAPT G2S mass spectrometer was used with a retrofitted MS™ inlet tube and an MS™ Ionique manual platform for SAI. Using an external power supply and heater, the inlet was brought to a temperature of 250 °C. Fused silica with a 100 μm I.D. was inserted 13 mm inside the inlet using the manual platform, and the solution was set to infuse at a rate of 50 μL min^{-1}.

2.8 | Use of a drift-tube instrument: MAI- and ESI-IMS-MS

The 2 m drift-tube instrument was used as described elsewhere.[67,68] Briefly, the source is based on the Smith ion funnel design[69] including the jet disrupter (Scheme S2, supporting information) for improvements in sensitivity and performance in ESI.[70–73] In order to use the instrument for MAI, the ESI source was removed to provide free access to the inlet which was not heated. The sample preparation conditions of 10^{-5} M ubiquitin solution in water/ACN/AA 49:49:2 (% v/v/v) and 50:50:0 (% v/v/v) were used as previously described.[59]

2.9 | Use of a Q-Exactive Focus instrument: MAI-, ESI-, and SAI-MS

Mass spectra were acquired on a Q-Exactive Focus mass spectrometer (Thermo Fisher Scientific, San Jose, CA, USA) interfaced with the MS™ Ionique manual platform after removing the Ion Max source with no inlet modification. MAI mass spectra were acquired using the syringe method in which 0.2 μL of 2 μM ubiquitin in 95% water/5% methanol with 100 ppm ammonium tartrate was mixed with 0.4 μL of an aqueous 3-NBN matrix solution containing 60% ACN and 100 ppm ammonium tartrate. This was dried on a 1-μL syringe needle tip before being inserted into the mass spectrometer inlet. In ESI, 1 μL of the ubiquitin solution was drawn into the 1-μL syringe and 3.5 kV applied to the syringe needle about 1 cm from the inlet aperture while the solution was slowly expelled to create a spray. In SAI, the same procedure was followed as with ESI, except that no voltage was applied and the syringe needle was placed inside the inlet tube with the tip against the inlet tube wall with expulsion of the solution. The instrument was tuned using ESI with settings which gave only low charge-state ions from the ubiquitin solution.

3 | RESULTS

3.1 | Commercial TWIMS instruments: LSI-, SAI-, and MAI-IMS-MS

ESI, SAI, LSI, and MAI all produce multiply charged ions of small proteins with excellent ion abundance from a variety of small molecule matrices when using a heated inlet tube. Only ESI requires application of high voltage to the solution at atmospheric pressure prior its entrance into the inlet. As a heated inlet tube is not standard on the Waters SYNAPT G2 and SYNAPT G2(S) IMS-MS instruments, modification of the skimmer cone inlet is necessary for optimum SAI, as well as for MAI, when using less volatile matrices.[32,37,44,50,51] Some of the inlet source developments are depicted in Scheme S1 (supporting information) and their relative operation and performance characteristics are also detailed in the supporting information. It is noteworthy that the commercial inlet geometries are significantly different between the SYNAPT G2 and the SYNAPT G2(S), in that the latter has extra pumping capacity and a collision surface built into the inlet which can be beneficial with the new ionization processes.[27,29,32] Both inlets are indirectly heated by the source block to a maximum of 150 °C. Additional heat may be applied using an external cartridge heater controlled with a power supply. Specific details for source conditions and results obtained are included in the supporting information (Figures S1 to S13). However, with certain more volatile solvents used with SAI and solid matrices in MAI, inlet modification is not necessary to achieve good ion abundance. With newly discovered spontaneously ionizing MAI matrices, the sample can be directly inserted into the instrument vacuum, even using the intermediate pressure MALDI sample plate and without the need to initiate the laser. Likewise, at atmospheric pressure on an overridden ESI source, sample can be introduced into the inlet aperture at ambient temperature using e.g. pipet tips (Figure S14, supporting information). Thus, there are a variety of configurations possible with the new ionization methods, and only a few are explored herein relative to ubiquitin structures. Nevertheless, we believe that the chosen approaches are fairly representative of what will be achieved with any configuration.

3.1.1 | Laserspray ionization (LSI)-IMS-MS

The same ubiquitin solution conditions (ACN/water/2% AA) used by Clemmer and coworkers for ESI-IMS-MS[4] were used to produce highly charged gaseous ubiquitin ions by ESI in the nanoESI source and LSI using the same SYNAPT G2 IMS-MS instrument. For LSI, the nanoESI source inlet was slightly modified according to a previously described protocol and the laser aligned in transmission geometry[34,50] using 2,5-DHAP as the matrix.[74] For ESI, a voltage of 3 kV was applied to initiate ionization. Other conditions, such as 150 °C source temperature and the default cone voltage setting of 40 V, were used for both ESI and LSI to provide the fairest comparison between the two ionization methods, although LSI does not require voltages be applied.[34,36,50] Typical two-dimensional (2-D) t_d versus mass-to-charge (m/z) datasets for ubiquitin ions obtained by LSI and nanoESI are shown in Figures S15B and S16B (supporting information), respectively. The charge-state distributions of the LSI ions range from +4 to +12 and the nanoESI ions from +5 to +13. The overall shift to higher charge states and higher signal abundance can be best seen in the total mass spectra displayed to the left of the respective 2-D plots. In ESI, higher charge states relate to more open (unfolded) structures,[54] and the same can be expected for LSI-, MAI-, and SAI-generated ions.

Detailed information on the relative structures of ions can be obtained from t_d-distributions extracted from the dataset by integration of narrow (isotopic) m/z regions for each charge state displayed in a 2-D plot. Figure S17 (supporting information) shows the t_d-distributions of ubiquitin charge states +4 to +12 for LSI (left panel, Figure S17A) and +5 to +13 for ESI ions (right panel, Figure S17B). The t_d-distributions are very similar for all charge states for both ionization processes. Charge state +5 produced by LSI and ESI shows a notably more compact structure than the +6 to +12 charge states, as reported previously for ubiquitin using electron-capture dissociation.[59] The ESI and LSI results follow the general trend of the t_d-measurements obtained for these charge states on a homebuilt IMS-MS instrument.[59] Some direct comparisons of ESI and MAI ionization methods using the IMS-MS homebuilt drift-tube instrument are included below. More detailed analyses reveal that charge states +7 to +12 have one significant, abundant feature, and charge states +5 and +6 show a number of low-abundance features. Differences are observed for the shape of the t_d-distributions in that LSI ions are generally slightly sharper (narrower) than those of the ESI ions, possibly suggesting fewer conformations, as shown by the +9 drift-time width of ~0.9 ms for LSI in comparison with ~1.3 ms for ESI (Figure S17, supporting information). In other studies using different conditions, multiple conformers were observed for these charge states.[26] For charge state +12, more resolved t_d-distributions for two abundant structures are observed for LSI-generated ions than for ions formed by ESI. Two distinct conformations have been previously described for the +12 charge state.[55] The close similarity of the t_d-distributions obtained with LSI using a solid matrix and ESI using a solvent with the same solution composition and instrumental parameters implies that the ions achieve common structures regardless of their initial gas-phase ion structure due to instrumental factors, or, seemingly less likely, that sufficient solvent is associated with the protein in LSI to create the same initial structures as ESI. The use of a laser does not appear to drastically influence the outcome of the t_d-distributions of the gaseous protonated proteins.

In the following experiment, we examined the changes occurring in LSI-generated ubiquitin ions under the influence of extraction voltages from 0 to 100 V. This provides information relative to energy supplied to the protein ions produced by LSI in an intermediate pressure region by application of a voltage (cone voltage) typically used for in-source fragmentation. The mass spectra are summarized in Figure S18 (supporting information). Under conditions of zero volts applied between the sample and the atmospheric pressure inlet for LSI and zero cone voltage, charge states +4 to +12 are observed.

Increasing the cone voltage increases the ion abundances, possibly because charged particles are better desolvated. Another observed trend is that the background increases between ~m/z 600 and 1200 which may be related to in-source fragmentation. In addition, the low charge states +5 and +6 especially increase in ion abundance (Figure S18, supporting information) with increasing voltage while the high charge states successively decrease in abundance with increasing voltage. This increase in the lower charge states may be because of charge stripping[75]; however, the decrease in the higher charge states can be either charge stripping or fragmentation. The highest abundance ion is +10 at zero cone voltage and +7 at 100 V. Similar to MALDI, it is not expected that the lower charge states under the high-energy conditions are related to more compact structures, as demonstrated below.

The integration of narrow (isotopic) m/z regions for charge states +5, +7, and +9 for ubiquitin acquired using LSI with increasing cone voltage, 0 to 100 V, using 2,5-DHAP as matrix, is summarized in Figure 1. The t_d-distributions of the LSI ions show different features for different charge states but follow the general trend of those of the nanoESI-generated ions (Figure S17B, supporting information). With *zero cone voltage*, in addition to one abundant feature, highly abundant more compact ubiquitin features are now observed, especially for charge state +7 (Figure 1B). The observation of more compact features at a cone voltage of 0 V indicates that this ionization is at least soft enough to produce these compact structures. Observing even more compact structures may be limited by the energetics supplied by the instrumentation. At a cone voltage of 20 V, the compact structures are reduced in abundance. Under default cone voltage conditions used with ESI (40 V, Figure 1), on this IMS-MS instrument, the more compact protein conformations are essentially destroyed with both ESI and LSI. Protein unfolding with increasing voltage is expected considering previous ESI-IMS-MS studies.[76]

These results also revive an interesting question relative to incorporation of the analyte in the matrix.[30,77,78] If the protein is co-crystallized within the matrix lattice at the point of application of voltage, how can a small increase in cone voltage alter conformations? This may indicate that a significant portion of analyte ions are free of matrix in the region where voltage is applied. This is most likely with relatively volatile matrices such as 3-NBN used here.[27,29–31,46,49] Alternatively, the protein may not be incorporated into the matrix crystal but reside on the surface in a manner where collisional or thermal energy can alter the conformation. Some evidence consistent with analyte residing on the matrix surface being sufficient for analyte (protein) ionization has been reported.[30]

The t_d-distribution of charge state +5 (charge stripped ions with increasing cone voltage, Figure 1A) is broad, and, as the ion abundance in the mass spectra increases (Figure S18, supporting information) along with the intensity of the t_d-distribution (cone voltage 60 to 100 V), the width of the t_d-distribution stays essentially unchanged compared with 0 V. This, together with essentially the same results for ESI and LSI acquired on the same mass spectrometer (Figure S17, supporting information), suggests that the many conformations observed in the t_d-distribution of charge state +5 are related to the propensity of the low charge state ions to spontaneously fold to stable structures in the time-frame of the experiment.[26] These comparisons show that, with the Waters SYNAPT mass spectrometers, the t_d-distributions and charge-state distributions achieved with LSI using a solid matrix and ESI using a solvent are closely similar.

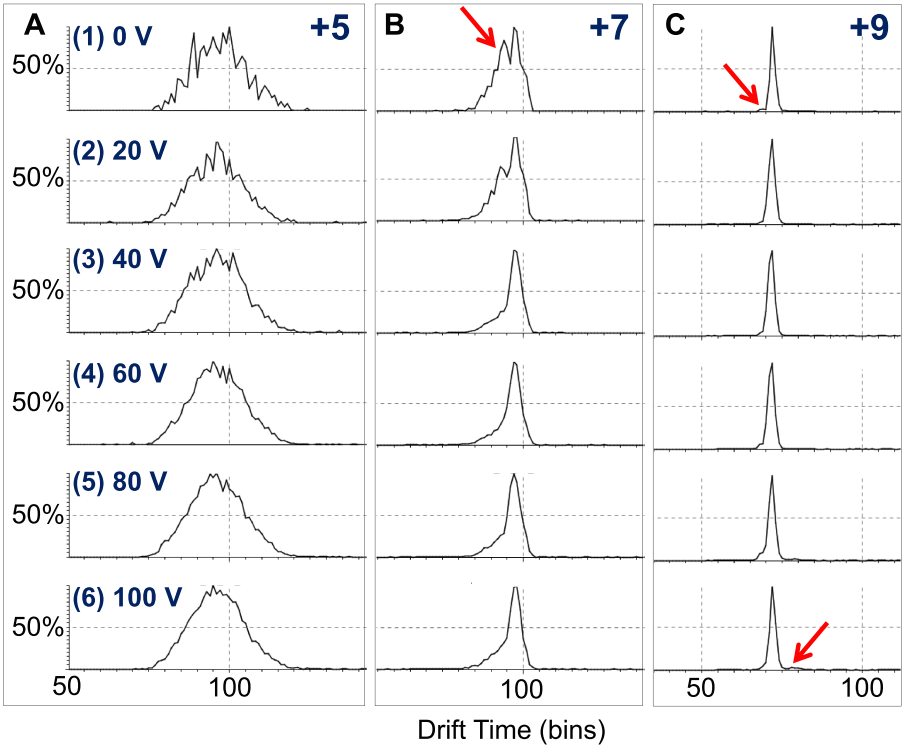

FIGURE 1 Extracted drift-time distributions of charge states: A, +5; B, +7; and C, +9 with different sample cone voltage: (1) 0, (2) 20, (3) 40, (4) 60, (5) 80; and (6) 100 V. Data were acquired using LSI-IMS-MS of ubiquitin (MW 8561 Da) in ACN:water:2% AA with 2,5-DHAP as matrix on the Waters SYNAPT G2 instrument. Full mass spectra are shown in Figure S18 (supporting information) [Color figure can be viewed at wileyonlinelibrary.com]

3.1.2 | Matrix-assisted ionization (MAI)-IMS-MS (no laser)

In LSI, ionization is initiated in the inlet and not by the laser[31–38,41,47,50,51]; therefore, the laser can be omitted. The discovery of matrices which spontaneously produce ions of the associated analyte without the need to apply heat has made the MAI method accessible with any mass spectrometer without inlet modification. One alternative is to insert the matrix with the associated analyte directly into the intermediate pressure on a substrate without passing through the inlet tube and without application of heat (*vacuum* MAI or *v*MAI). Two methods are available for *v*MAI: one inserting the sample using the intermediate pressure MALDI plate introduction mechanism without initiating the laser, and the other using a probe device to insert the sample into vacuum just in front of the inlet to the mass analyzer. Ionization occurs spontaneously using these two methods on either the SYNAPT G2 or the SYNAPT G2S mass spectrometer. With *v*MAI, using 3-NBN as the matrix dissolved in 100% ACN and ubiquitin in ACN/H_2O ranging from 25 to 90% aqueous mixed 1:1 v/v, the mass spectra and t_d-distributions are quite similar, as shown for charge state +11 (Figure S19, supporting information). However, using ubiquitin in 90% water and 10% ACN, the *v*MAI t_d-distributions on the commercial intermediate pressure MALDI source of the SYNAPT G2S without initiating the laser (Figure 2A) show more compact features than ESI from atmospheric pressure using default setting on the SYNAPT G2. A comparison of vMAI (Figure 2B) with ESI (Figure 2C) on the SYNAPT G2 for ubiquitin in 100% water mixed with 3-NBN in 100% ACN for MAI, and for ESI, 90% water and 10% ACN, shows essentially the same t_d-features for charge states +5 to +10, but a somewhat more abundant compact structure for +11 using *v*MAI (Figure 2B). Nevertheless, it is surprising that spontaneous ionization from a solid matrix in vacuum gives nearly identical t_d-distribution to ESI from atmospheric pressure unless the energy input from ionization and instrumentation exceeds the threshold necessary for rearrangement to stable conformers.

A significant issue relative to native MS is that 3-NBN is insoluble in water. Only a couple of the self-ionizing matrices discovered so far dissolve in 100% aqueous solution. One of them is MNP.[46] A comparison of experimental conditions such as solvents, matrices, and temperature was performed with the 100% aqueous solution of both the analyte and the MNP matrix, as well as with 90% water:10% ACN, and a binary mixture of MNP and 3-NBN in this solvent, all with the inlet at 30 °C. These results were compared with those from ESI in 90% water:10% ACN with the inlet at 80 °C. The t_d-distributions of the +7 charge state of ubiquitin for these solutions, inlet temperatures, and default instrument settings for ESI are displayed in Figure 3. Also included in Figure 3 are the +7 charge-state t_d-distributions using MAI with 3-NBN as matrix in ACN with analyte in 90% water:10% ACN at 30 °C, and the results for LSI with the same matrix and solution conditions at inlet temperatures of 30 and 80 °C. All measurements were acquired on the SYNAPT G2. In more detail, the t_d associated with the MNP matrix at 30 °C, where the solution is at least 90% aqueous (Figures 3A and 3B), shows the most compact structures. The matrix 3-NBN, pure or as a binary mixture with the matrix MNP, at low inlet tube temperatures (Figures 3C and 3D) provides two more relatively well-defined t_d's for charge state +7

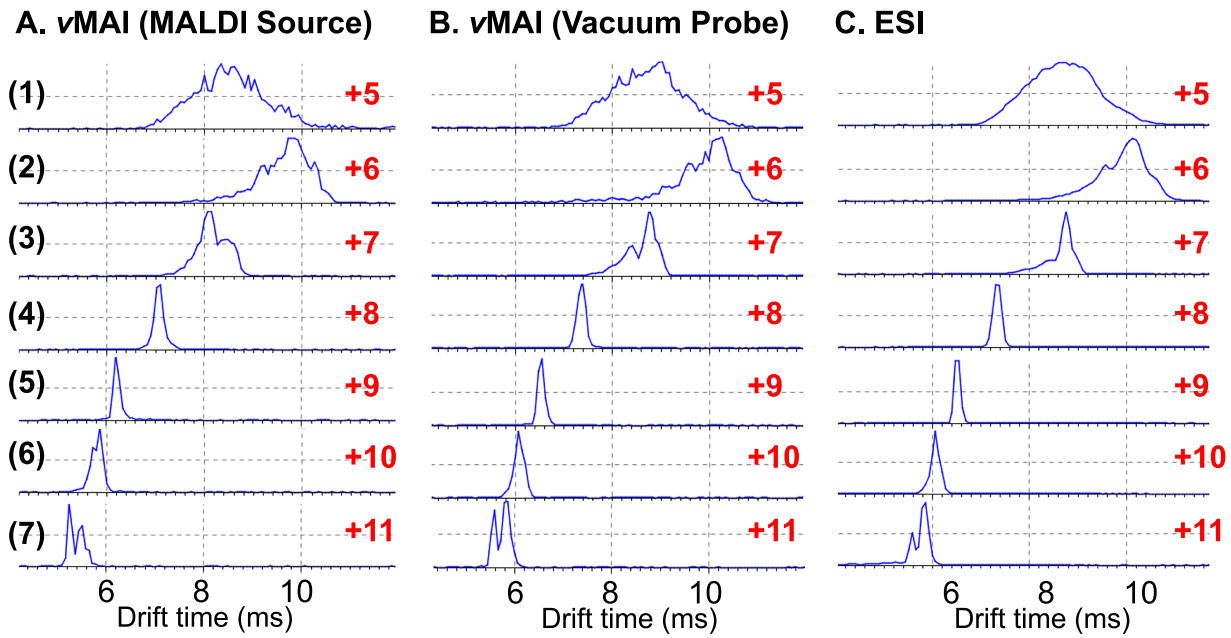

FIGURE 2 Extracted drift times of ubiquitin in 90% water:10% ACN mixture: MAI-IMS-MS with 3-NBN matrix in 100% ACN using: A, *v*MAI on a commercial intermediate pressure MALDI source without initiating the laser; B, *v*MAI using the vacuum probe; and C, the commercial Waters ESI-IMS-MS instrument using default settings (80 °C source temperature, 40 V cone voltage and 3.5 kV capillary voltage). Data acquired using A, the Waters SYNAPT G2S and B, C, the G2 instruments. Representative mass spectra are shown in Figure S20 (supporting information) [Color figure can be viewed at wileyonlinelibrary.com]

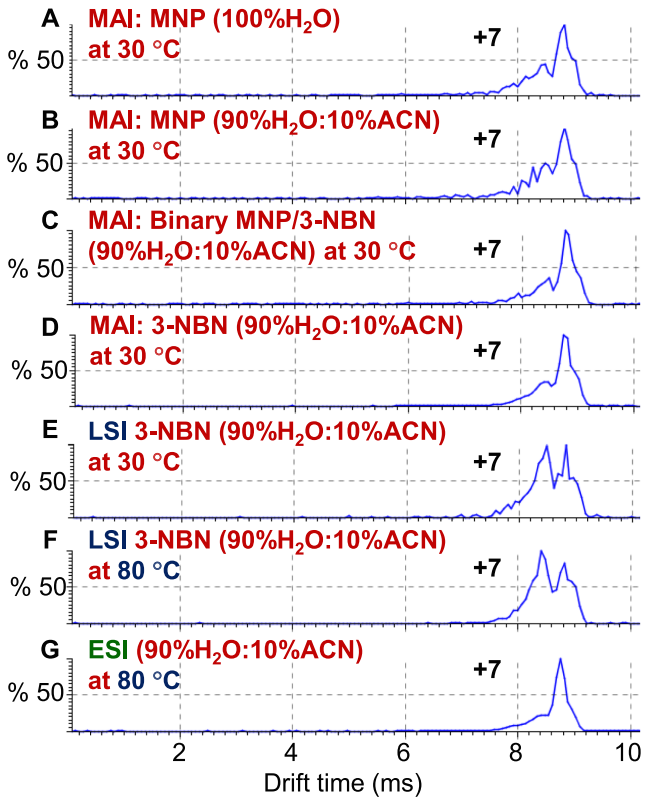

FIGURE 3 Extracted drift-time comparison of the +7 charge state of ubiquitin using: A, MAI with MNP (100% water); B, MAI with MNP (90% water:10% ACN); C, MAI with binary matrix MNP:3-NBN (90% water:10% ACN); D, MAI with 3-NBN (90% water:10% ACN); E, LSI with 3-NBN (90% water:10% ACN) at 30 °C; F, LSI with 3-NBN (90% water:10% ACN) at 80 °C; and G, ESI (90% water:10% ACN). Data acquired on the Waters SYNAPT G2 instrument at 30 °C source temperature using MAI (A, B, C, D) and sample was introduced using a pipette tip; (E, F) LSI (337 nm N_2 laser) and sample on a glass plate (note, 3-NBN matrix has absorption at 266 nm[43]) and (G) ESI using default settings with 40 V cone voltage and 80 °C source temperature. Representative mass spectra are shown in Figure S20 (supporting information) [Color figure can be viewed at wileyonlinelibrary.com]

which become more pronounced with the use of a laser and with higher (80 °C) source block temperature (Figures 3E and 3F). The unexpected abundant feature of what appears to resemble "compact structures" (t_d ~8.5 ms) is seen using 3-NBN matrix and a laser (Figures 3E and 3F). If the LSI-generated protein ions are laser activated, one would expect more elongated structure(s) unless the ions detected are collapsed structures. It is clear that the laser has an effect on the +7 charge-state ion although the laser is not responsible for the ionization process. Thus, the ubiquitin molecule, possibly embedded within the matrix,[30,32,78] appears to be structurally altered by the energy from the absorption of the 337 nm N_2 laser beam which may be directly through the protein (note, 3-NBN has a strong absorption at 266 nm but not at 337 nm[43]). As a reference, the fewest structural features within these direct comparisons of various conditions are observed for ESI with the default conditions (40 V cone voltage) using 90% water and an inlet temperature of 80 °C (Figure 3G). This may suggest that the ubiquitin ions originating from 10% organic solution are retaining more of the aqueous solution structure using MAI with the water-soluble MNP matrix (Figure 3B) and with the 3-NBN matrix (Figure 3D) than using ESI with the higher energy default conditions (Figure 3G). The IMS resolution is too low to extract any further information. However, it is clear that the matrix, solution conditions, and ionization method used are not providing a large difference in conformations of the +7 ion with this instrument, except in the case where a laser is used. The mass spectral data is summarized in Figure S20 (supporting information). Charge-state distributions range from +5 to +11 with MNP as matrix (Figures S20A–20C) and up to +13 with 3-NBN as matrix (Figures S20D–20F). The charge-state distributions suggest mostly extended structures. Direct comparison of the t_d-distributions for charge states +5 in Figure S21 (supporting information) shows no statistical differences but, for charge states +11 (Figure S22, supporting information), an abundant feature is observed at t_d ~5.6 ms for MAI and LSI in comparison with ESI.

Differences in the compact features are observed with *v*MAI using the intermediate pressure MALDI source without the laser. A comparison of the +11 charge-state t_d-distributions is shown in Figure 4. The SYNAPT G2S (Figure 4A) shows the most abundant compact feature relative to measurements of *v*MAI using the *vacuum*-probe (Figure 4B), MAI (Figure 4C) and LSI from atmospheric pressure

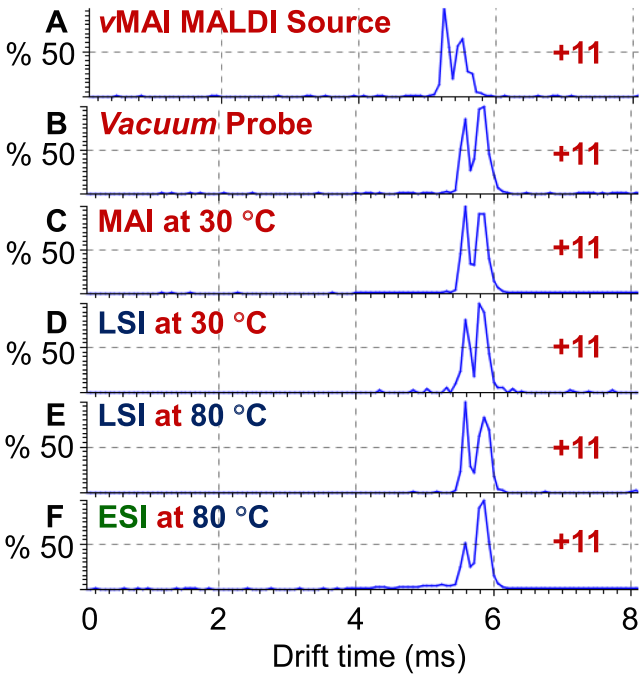

FIGURE 4 Extracted drift time of the +11 charge state of ubiquitin in 90% water:10% ACN with 3-NBN matrix using: A, *v*MAI (MALDI source); B, *v*MAI (*vacuum*-probe); C, MAI; and D, LSI at 30 °C (337 nm N_2 laser) with the matrix having absorption at 266 nm;[43] E, LSI at 80 °C; and F, ESI using default settings with 40 V cone voltage and 80 °C source temperature. Data acquired on A, the Waters SYNAPT G2S and B, C, D, E, F, the G2 instruments. Representative mass spectra are shown in Figure S20 (supporting information) [Color figure can be viewed at wileyonlinelibrary.com]

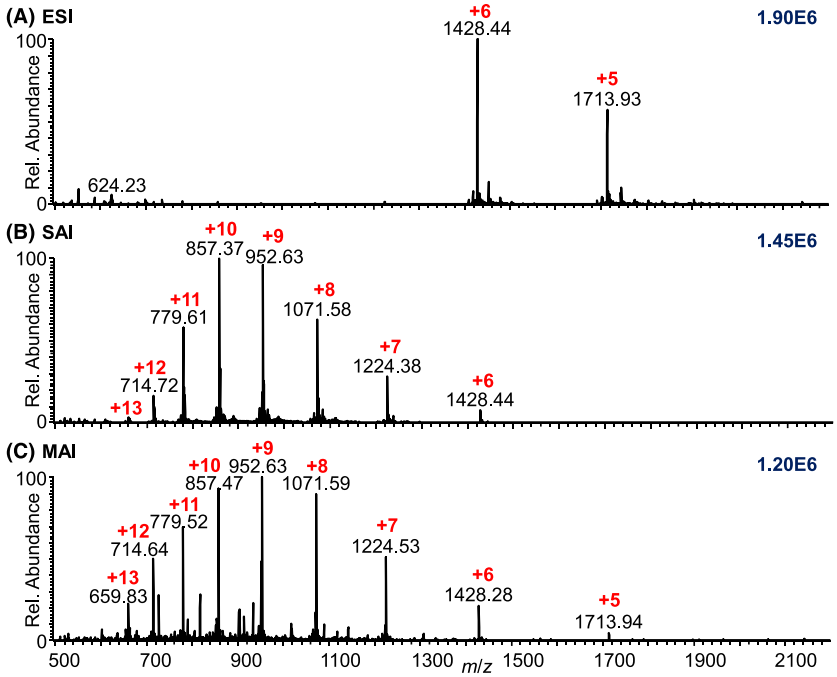

FIGURE 5 Mass spectra of ubiquitin (5 μM) in 100 ppm ammonium tartrate containing 5% methanol acquired using the manual Ionique platform on a Thermo Q-Exactive Focus mass spectrometer (Thermo Fisher Scientific): A, ESI; B, SAI; and C, MAI [Color figure can be viewed at wileyonlinelibrary.com]

(Figures 4D and 4E), and ESI (Figure 4F) acquired on a SYNAPT G2; for Figures 4A–4E the matrix 3-NBN was used. Interestingly, ESI (Figure 4F) shows the least abundant compact conformation, but this is attributed to using the default settings which impart significant energy into the ions, especially from the 40 V cone voltage and the 80 °C inlet temperature. Note that the t_d-offset in Figure 4A relates to use of the SYNAPT G2S instead of the SYNAPT G2 (Figures 4B-F). For direct comparison, measurements by MAI at atmospheric pressure and *v*MAI using the intermediate pressure MALDI source and *vacuum*-probe were acquired using the SYNAPT G2S (Figure S23, supporting information). *v*MAI using the intermediate pressure MALDI source shows more of the compact features than MAI from atmospheric pressure and *v*MAI using the *vacuum*-probe which shows fewer compact features. For *v*MAI using the *vacuum*-probe, fewer compact features are observed for charge states +5 and +11 on the SYNAPT G2S (Figure S23C, supporting information) than on the G2 (Figures 2B and 4B).

3.1.3 | Comparison of charge-state distributions between ESI, SAI, and MAI

The charge-state distributions of ubiquitin were examined under conditions favorable for the ionization of folded structures; namely, the solution consisted of ubiquitin (5 μM) in 100 ppm ammonium tartrate containing 5% methanol. All mass spectra were acquired on a Thermo Fisher Scientific Q-Exactive Focus under conditions optimized for achieving low charge states by ESI. For ESI and SAI, the inlet capillary was set at 250 °C and with MAI at 100 °C. All other settings were the same where applicable for ESI, SAI, and MAI. The mass spectra are shown in Figure 5 and represent an average of ten 0.5 s acquisitions at a mass resolution of 70,000, $m/\Delta m$ 50% valley at m/z 200. The ESI mass spectrum displayed in Figure 5A shows almost exclusively charge states +5 and +6 while the SAI and MAI mass spectra show charge states ranging from +5 to +11 (Figures 5B and 5C). The high charge states for MAI were not surprising since the matrix solution which was combined with the ubiquitin solution 3:1 was in 100 ppm ammonium tartrate solution containing 60% ACN. However, the SAI and ESI solutions were the same, as were all other conditions, with the exception that the ESI spray is at atmospheric pressure with voltage while in SAI the solution flows through capillary tubing directly into the inlet tube where ionization occurs at sub-atmospheric pressure. While both ionization methods are believed to operate from charged droplets, the mass spectra are drastically different (Figures 5A and 5B). It is tempting to think that the difference relates to heat transferred by the inlet, but in thermometer ion studies comparing ESI and SAI, SAI produced less fragmentation.[79] Furthermore, Johnston's group demonstrated that inlet temperatures >800 °C did not cause thermal decomposition in droplet ionization, a variant of SAI.[42] However, in retrospect, the thermometer ion study is not at odds with the results here and fragmentation requires significantly more energy than denaturing ubiquitin. The stated reason for SAI producing less thermometer ion fragmentation than ESI was

that in ESI the ion is mostly desolvated before the heated inlet tube and thus experiences the heat from the inlet, whereas, in SAI, the solvent is present through most of the inlet tube, thus protecting the ion from thermal degradation. In the case of charge states of a protein, the charge state observed cannot be increased after leaving the droplet, but additional energy input can occur and alter the conformation.[80] In ESI, the protein is mostly desolvated before the heated inlet and maintains a folded structure and thus low charge states, whereas, in SAI, the results are best explained by the inlet heating the droplet thus denaturing the protein. However, in both cases, the ions observed will experience energy input from the inlet temperature and voltages applied in regions where collisions with gases occurs. Thus, whereas in SAI the bare ions are more unfolded than in ESI, the final energy of the ions when passing through the IMS region may be more energetic in ESI under similar experimental conditions.

Similar comparisons of ionization methods and solvent compositions were performed on the Waters SYNAPT G2S IMS-MS instrument to examine charge states and t_d-distributions. Formic acid, 0.1%, in a 5 μM solution of ubiquitin in aqueous 5% methanol was first used because of the ability to ionize by SAI at relatively low inlet tube temperatures.[32] In addition to the commercial Waters LockSpray ESI source, the source of the Waters instrument was retrofitted with an MS™ inlet tube and the manual multifunctional Ionique platform to implement the use of *inlet* ionization. Good ion abundance was observed for all *inlet* and *vacuum* ionization methods and ESI using the Waters ESI source (Figure S25, supporting information). The experimentally observed charge states for ESI (Figure S25A, supporting information), SAI (Figure S25B(2), supporting information), MAI (Figure S25B(3), supporting information), and *v*MAI (Figure S25C, supporting information) are the high charge states, typically ranging from +4 to +13. Of these, ESI provided a bimodal charge distribution from +4 to +6 and +7 to +10, as did *v*MAI from +5 to +6 and +7 to +13, possibly corresponding to the presence of various degrees of folding. There are many interesting similarities associated with the t_d-distributions observed throughout all four of the different ionization methods. Mainly, the lower charge states exhibit broad t_d-distributions, some of which are asymmetric, such as the +6 charge state observed in ESI (Figure S25A, supporting information) and *v*MAI (Figure S25C, supporting information), where the majority of the area lies towards the higher t_d's. Characteristic t_d-distributions are observed for +7 and +11 charge states with the exception of MAI.

Secondly, buffered sample preparation conditions, 5 μM ubiquitin in aqueous 5% methanol containing 100 ppm ammonium tartrate, were subsequently used on the SYNAPT G2S. The commercial Waters ESI source provided a bimodal distribution of charge states ranging from +5 to +8 and+9 to +12 (Figure 6A). The multi-ionization MS™ Ionique manual platform was subsequently used. First, ESI with a flow rate of 10 μL min^{-1} and 3.5 kV applied to a metal union linking fused-silica tubing resulted in primarily +5 and +6 charge states (Figure 6B(1)). The results are similar to those using the Thermo Q-Exactive Focus (Figure 5A) and reported for nanoESI using the Waters nanoESI source and an ammonium acetate buffered solution.[63]

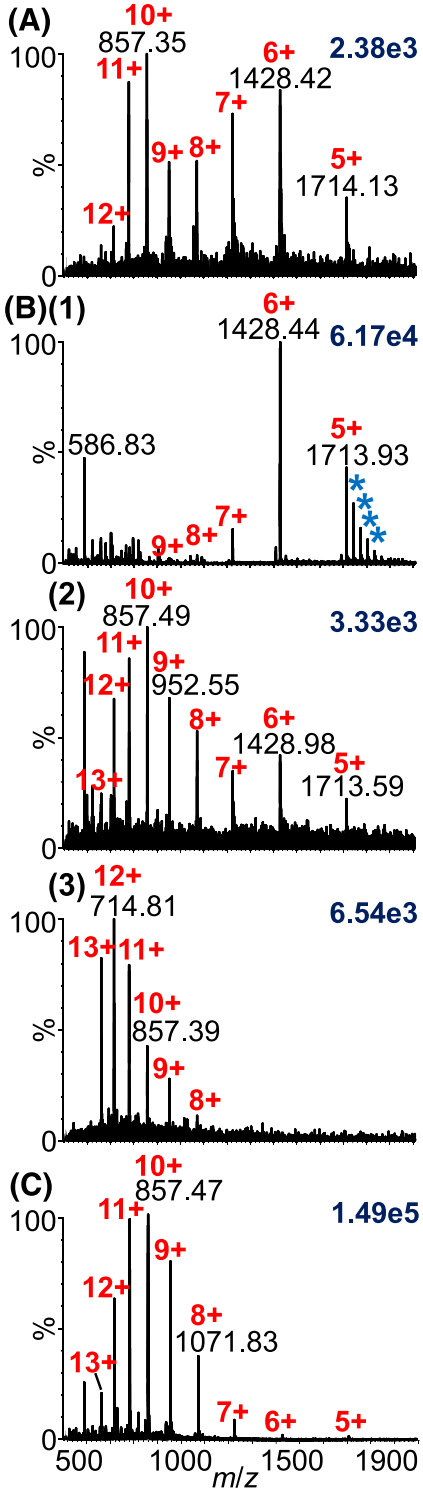

FIGURE 6 Comparison of mass spectra showing relative abundances of various charge states of aqueous 5 μM ubiquitin buffered with 100 ppm ammonium tartrate containing 5% methanol. Data acquired on a Waters SYNAPT G2S using different sources and platforms: A, the commercial Waters ESI source; B, the MS™ manual Ionique platform [(1) ESI, (2) SAI, (3) MAI]; and C, the MS™ *v*MAI *vacuum*-probe. Multiple tartaric acid adductions (*) are apparent for charge state +5 as shown in B(1). Extracted drift times are shown in Figure S26 (supporting information) [Color figure can be viewed at wileyonlinelibrary.com]

Multiple tartaric acid adductions were apparent in charge state +5 and to a lesser degree in +6 (Figure 6B(1)). This carboxylic acid adduction to ubiquitin has been reported for ammonium carboxylate buffered ESI studies and accounts for a significant amount of protein ion abundance under these 'native' ESI conditions.[62] Second, using the same MS™ platform and ammonium tartrate buffered solution of ubiquitin, SAI provided a bimodal charge-state distribution ranging from +5 to +7 and +8 to +13 (Figure 6B(2)), respectively, while undesired tartaric adductions were not observed. Although both MS™ SAI (Figure S26B(2), supporting information) and Waters ESI (Figure S26A, supporting information) showed a bimodal distribution, the relative abundance of the lower charge states is higher in ESI than in SAI. Third, MAI showed high charge states ranging from +8 to +13 (Figure 6B(3)), while *v*MAI using the homebuilt *vacuum*-probe[52] showed charge states ranging from +5 to +12, and exhibited significantly less background (Figure 6C). Buffered conditions appear to be helpful in SAI for observing lower charge-state ions (Figure 6B (2)), but not (yet) for MAI under the conditions used here. Interestingly, charge state +6 observed using SAI with buffered conditions shows a higher abundance of more folded conformations than *v*MAI and ESI using the commercial source, but similar to ESI using the MS™ manual platform (Figure S26B(1), supporting information). As stated before, bimodal charge-state distributions were noticed in ESI (Figure S25A, supporting information) and *v*MAI (Figure S25C, supporting information) acquisitions under acidic conditions, as well as in ESI (Figure 6A) and SAI (Figure 6B(2)) under buffered conditions.

Extracting the t_d-distributions shows intriguing similarities and minor differences. These are summarized according to their +5, +7, and +11 charge states as seen in Figure 7. The broad +5 charge state appears 'jagged' when acquired with the commercial Waters ESI source (Figure 7A), the MS™ platform using SAI (Figure 7B(2)) and *v*MAI (Figure 7C). However, the +5 charge state appears 'smooth' with the MS™ platform using ESI (Figure 7B(1)). This appears to be related to the relatively high total ion abundance of 6.17e4 (Figure 6B (1)) counts obtained for ESI on the MS™ platform. Thus, the 'jagged' t_d-appearance is probably due to statistical fluctuations because of low ion abundance of this charge state rather than different conformations.

Direct comparison of +5 and +7 charge-state t_d-distributions of ESI using different sources and solvent systems (Figure S27, supporting information) shows a similar 'jagged' t_d-appearance of the low-abundance +5 charge state (Figure S27A(1), supporting information) and no difference in the +7 t_d-distribution using the commercial ESI source (Figure S27A(2), supporting information). An obvious difference can be observed using the commercial ESI source (Figure S27A, supporting information) and the MS™ platform (Figure S27B, supporting information). The +5 and +7 charge states using the MS™ platform both show t_d-distributions towards a more compact feature than the commercial ESI source. Using different sources and platforms (Figure 7), a split t_d-distribution is observed in the +7 and +11 charge states, as was observed in Figures 3 and 4. Interestingly, the MAI t_d-distributions (Figure 7B(3)) do not show this behavior. Importantly, both SAI and ESI form lower charge states than MAI. This seems to indicate that the protein structures, based on the similar t_d-distributions observed for ESI and SAI, are essentially the same, at least on this commercial IMS-MS SYNAPT G2S instrument.

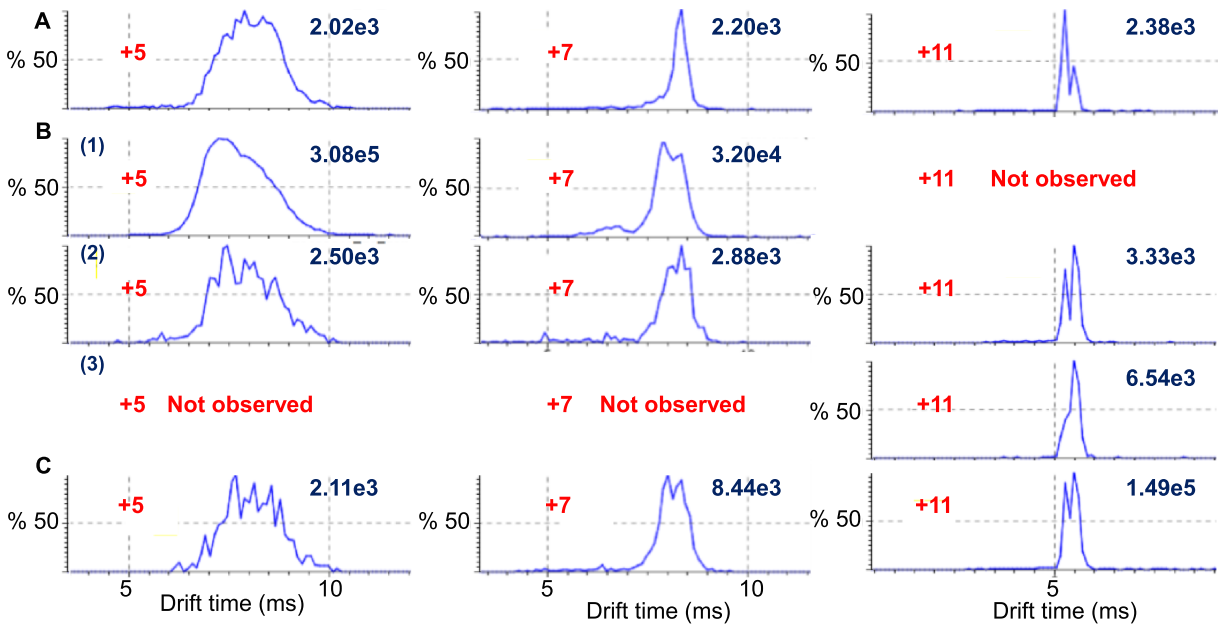

FIGURE 7 Extracted drift times of the +5, +7, and +11 charge states of ubiquitin (5 μM) in 100 ppm ammonium tartrate containing 5% methanol using different sources and platforms: A, commercial Waters ESI source; B, the MS™ manual Ionique platform [(1) ESI, (2) SAI, (3) MAI]; and C, the MS™ *v*MAI *vacuum*-probe. Data acquired on a Waters SYNAPT G2S. Additional extracted drift times are shown in Figure S26 (supporting information). Refer to Figure 6 for full mass spectra [Color figure can be viewed at wileyonlinelibrary.com]

3.2 | Use of a homebuilt 2 m drift-tube instrument: MAI- vs ESI-IMS-MS

Only minor differences in structural features of ubiquitin ions were observed between those generated by ESI and MAI with three different matrices and various solution conditions on the SYNAPT instruments. In order to determine if these results relate to the instruments rather than the ionization methods and solution conditions, IMS-MS results were acquired on the 2 m drift-tube instrument with ion funnel technology in Prof. Clemmer's lab. With this instrument, an obstruction is configured within the ion funnel with the purpose of disrupting any remaining ESI droplets.[69–73]

Observation of protein ions using 3-NBN as matrix with this instrument showed a strong preference for the matrix:analyte sample being introduced in solution into the short non-heated inlet opening instead of as the dry matrix:analyte sample which is typically used with commercial mass spectrometer inlets that can be heated.[46,66] There was a delay of approximately 15 s before protein ions were detected in a short strong 'pulse-like' ion burst, contrary to the operation using the commercial instruments and inlets. It is reasonable to assume that the wet sample collects inside the sub-atmospheric pressure side of the IMS-MS inlet, more specifically on the jet disrupter.[73] We envision that in MAI, under these sub-atmospheric pressure conditions, the wet sample freeze dries. After the matrix:analyte sample is sufficiently dry, a burst of ion current is detected similar to what is observed when the matrix is crushed in vacuum to produce small matrix particles.[30,53] This suggests the possibility that sudden solvent expansion may produce small matrix particles which rapidly sublime to produce the burst of analyte ions. Unfortunately, because of this difference relative to MAI on the SYNAPT G2S, comparisons of results are not necessarily straightforward. The results may be more closely aligned with those obtained on the intermediate pressure MALDI source of the SYNAPT instruments. The MAI matrix:analyte sample is introduced dry on a sample plate[31,49] or on a probe[27,30,52] directly into vacuum. The ion duration without the use of a laser can be as long as 30 min using the 3-NBN matrix,[49,78,81] but an intense burst of ions is produced by crushing the sample.[30,53]

While various matrices have been tested on the homebuilt IMS-MS instrument, only the better performing MAI matrix 3-NBN was useful with this instrument (Figure S28, supporting information). This too is different from the commercial vacuum source where over two dozen MAI matrices support analyte ionization from small drug molecules to proteins.[31,46,49] MAI matrices that are soluble in 100% water are less volatile than the 3-NBN matrix, and would require improved *inlet* and *vacuum* ionization conditions to be operational on the homebuilt IMS-MS instrument. These failures with less volatile matrices suggest the need for an inlet tube, preferably being heated, for this ESI-configured instrument.[32,37,44,45,50,51,78] While absorption of the laser beam can impart surface heat, this does not serve as a substitute for a heated inlet tube, similar to previous findings,[32,47,50,51] at least not for nonvolatile compounds. Low-abundance ions of small molecules have been observed on this homebuilt instrument using a less volatile matrix and a laser (Figure S28, supporting information).

Charge states +7 to +15 are observed (Figure 8A) from wet 3-NBN matrix:ubiquitin sample introduction into the unheated inlet. Interestingly, a bimodal charge-state distribution is observed with the most abundant charge states at +12 and +9. Bimodal distributions have previously been observed under *vacuum* ionization conditions using 2-nitropholoroglucinol matrix, but not with atmospheric pressure introduction.[32,82] The extracted t_d-distributions are shown in Figure 8B displayed by cross-sections of ubiquitin. Published ubiquitin work using the ESI method with a similar homebuilt drift-tube instrument, but 3 m long, shows similar cross-sections for charge states +7 to +13; charge states +14 to +16 were not reported in the

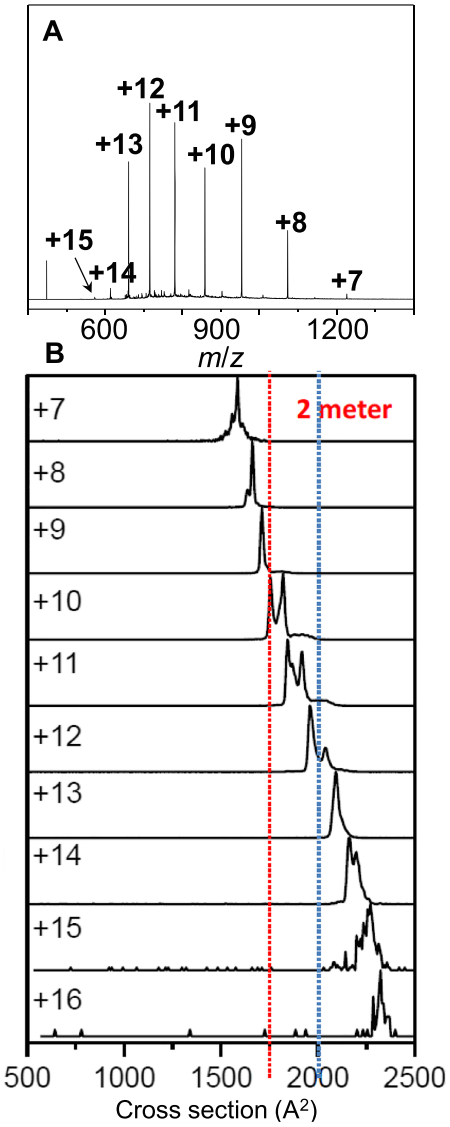

FIGURE 8 MAI-IMS-MS of ubiquitin in 90:10 water:MeOH (pH 2) with 3-NBN matrix in 100% ACN: A, total mass spectrum and B, collisional cross-section (CCS) of the multiply charged ions +7 to +16. Data acquired using the homebuilt 2 m drift-tube instrument in Clemmer's laboratory at Indiana University [Color figure can be viewed at wileyonlinelibrary.com]

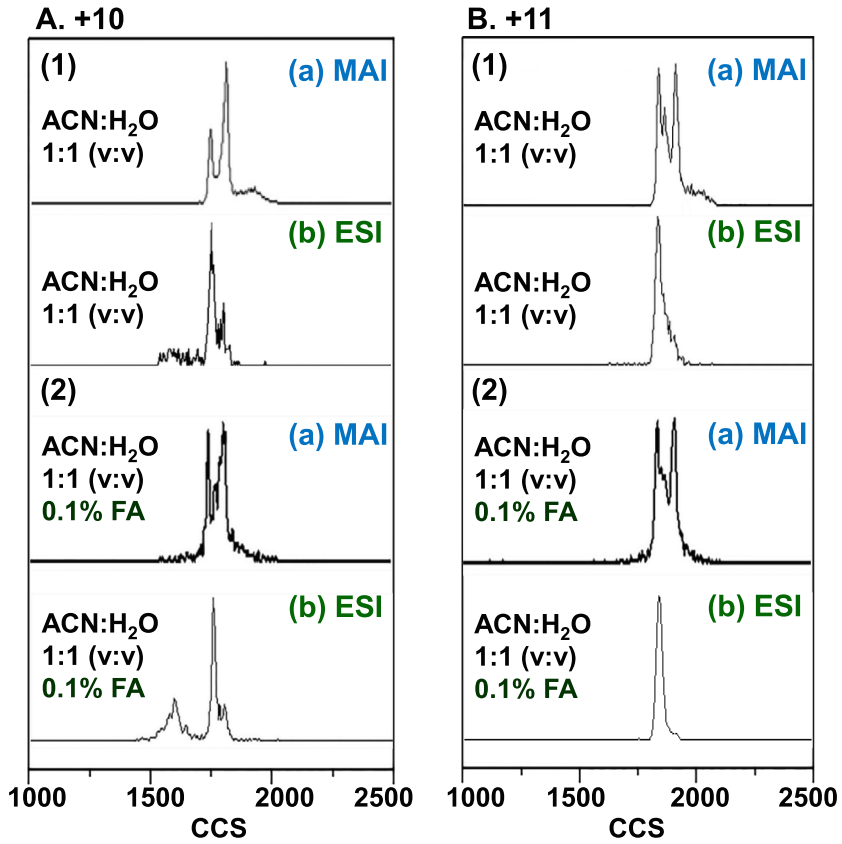

FIGURE 9 Analyses of collisional cross-section (CCS) of ubiquitin charge state: A, +10 and B, +11 from different solvent conditions (1) 1:1 acetonitrile (ACN):water (v/v) and (2) 1:1 acetonitrile:water (v/v) with 0.1% formic acid (FA) using (a) MAI-IMS-MS with 3-NBN matrix and (b) ESI-IMS-MS. Data were acquired using the homebuilt 2 m drift-tube instrument in Clemmer's laboratory at Indiana University [Color figure can be viewed at wileyonlinelibrary.com]

prior work.[59] There are three obvious differences between these measurements on two different mass spectrometers and two different ionization methods. First, charge states +5 and +6 were not detected with MAI on the 2 m drift-tube instrument. In ESI, these are the charge states that provide the compact structures at about 1100 Å^2 using the 3 m drift-tube instrument.[59] Secondly, while charge state +7 is detected in both datasets, with MAI, the observed cross-section is about 1600 Å^2 (elongated) while, with ESI, it is about 1100 Å^2 (compact). Thirdly, partially folded structures are not observed with MAI, although observed for charge states +8 to +10 with ESI in a size range from *ca* 1100 to 1700 Å^2. We partially attribute these differences to the solution conditions used where, for ESI, conditions more favorable to preserving folded structures were employed. With MAI using 3-NBN, the matrix preparation must use a relatively high organic solvent (acetonitrile) concentration to dissolve the matrix, so that observation of extended structures is not unexpected. The results for MAI on the 2 m drift tube instrument, for the charge states observed, look more similar to those obtained on the SYNAPT G2S with MAI or ESI, which probably relates to both solution conditions and the energy input by the instrument conditions used in the experiment.

Because of the difficulty of comparison between two different homebuilt instruments using two different ionization conditions, direct comparisons between MAI and ESI using two solvent conditions of ubiquitin in water:ACN (1:1) and water:ACN:acetic acid (49:49:2 by % volume) were performed (Figure 9). The conditions selected were based on previous work.[59] The extracted t_d-distributions are shown for charge states +10 (Figure 9A) and +11 (Figure 9B) with MAI (top, self-ionizing 3-NBN matrix) and ESI (bottom, 3 kV ionizing voltage). In all cases, MAI produces more abundant extended conformations (~1800 Å) and fewer of the most compact structures (~1600 Å) than ESI. These results are the first to show, under the most similar conditions applicable at this time, that the conformations observed are affected by the ionization method. The MAI results for charge state +11 look very similar, with the exception of better t_d-resolution on the 2 m instrument, than for *v*MAI on the SYNAPT G2 at intermediate pressure, and obtained under similar (Figures 2A and 2B, 4A and 4B) as well as different solution conditions (Figure S19, supporting information). Comparison of the +11 charge-state t_d-distribution acquired with MAI at atmospheric pressure (Figure S23A, supporting information) and *v*MAI using the *vacuum*-probe (Figure S23C, supporting information) shows that *v*MAI increases the contribution of the extended conformation suggesting higher energy conditions, which may relate to more efficient collisional cooling with *inlet* ionization. Although these results suggest that the matrix is involved in the degree of unfolding observed, a more definitive answer awaits an inlet tube entrance being provided onto the homebuilt IMS-MS instrument so that water-soluble matrices can be used.

4 | CONCLUSIONS

Comparisons between ESI and MAI using different solvents, solid and liquid matrices, and ion formation at different pressures show that the

t_d-distributions of ubiquitin multiply charged ions are essentially the same under commonly used operating conditions of energy input. Only when the energy input into the ions from voltages and heat is minimized, which was best accomplished with a homebuilt IMS-MS instrument, are differences in t_d-distributions related to the ionization method observed. Use of a solid matrix, as in MAI operating under sub-atmospheric pressure, produces a higher abundance of extended structures than in ESI with ionization initiated at atmospheric pressure using the same solution and instrument conditions. Although not definitive, the different pressure conditions for ionization suggest differences in the final desolvation states of the protein ions using solid *vs* liquid matrices. In addition, low charge states indicative of folded structures, while observed in ESI of ubiquitin, have so far not been observed with solid matrices including MNP which is soluble in 100% water. None of the ionization methods including ESI observed the compact structures observed with the homebuilt IMS-MS instrument including the conditions that led to the detection of the low charge states with the SYNAPT G2(S).

ACKNOWLEDGEMENTS

Funding from Wayne State University (CBL, EDI, ST), NSF CAREER 0955975 and CHE (CMI)-1411376 grants, ASMS Research Award (Waters Company), Eli Lilly and Company Young Investigator Award in Analytical Chemistry, and DuPont Company Young Professor Award is acknowledged. Doctors Mike Morris and Jeff Brown (Waters and its COI program) are kindly acknowledged for discussions about the potential path forward to convert the limited skimmer source inlet into an *inlet* ionization source. The authors thank Prof. McEwen (USciences) for access to the Thermo Q-Exactive Focus commercially equipped with a heated inlet tube, and MS™ for use of the Ionique manual platform for the ubiquitin studies. The authors are also grateful for the generous support from NSF STTR Phase II 1556043 including TECP and NSF SBIR Phase I 1913787. Any opinions, findings, and conclusions or recommendations expressed in this material are those of the authors and do not necessarily reflect the views of the National Science Foundation.

ORCID

Ellen D. Inutan https://orcid.org/0000-0003-4777-1737
Dean R. Jarois https://orcid.org/0000-0001-5293-0013
Christopher B. Lietz https://orcid.org/0000-0002-9682-6004
Tarick J. El-Baba https://orcid.org/0000-0003-4497-9938
Casey D. Foley https://orcid.org/0000-0002-8828-8808
David E. Clemmer https://orcid.org/0000-0003-4039-1360
Sarah Trimpin https://orcid.org/0000-0002-3720-2269

REFERENCES

1. Whitehouse CM, Dreyer RN, Fenn JB. Electrospray interface for liquid chromatographs and mass spectrometers. *Anal Chem*. 1985;57 (3):675-679.
2. Fenn JB, Mann M, Meng CK, Wong SF, Whitehouse CM. Electrospray ionization for analysis of large molecules. *Science*. 1989;246:64-67.
3. Valentine SJ, Anderson JG, Ellington AD, Clemmer DE. Disulfide-intact and reduced lysozyme in the gas phase: Conformations and pathways of folding and unfolding. *J Phys Chem B*. 1997;101: 3891-3900.
4. Valentine SJ, Counterman AE, Clemmer DE. Conformer-dependent proton-transfer reactions of ubiquitin ions. *J Am Soc Mass Spectrom*. 1997;8:954-961.
5. Li J, Taraszka JA, Counterman AE, Clemmer DE. Influence of solvent composition and capillary temperature on the conformations of electrosprayed ions: Unfolding of compact ubiquitin conformers from pseudonative and denatured solutions. *Int J Mass Spectrom*. 1999; 185/186/187:37-47.
6. Segev E, Wyttenbach T, Bowers MT, Gerber RB. Conformational evolution of ubiquitin ions in electrospray mass spectrometry: molecular dynamics simulations at gradually increasing temperatures. *Phys Chem Chem Phys*. 2008;10(21):3077-3082.
7. Koeniger SL, Merenbloom SI, Sundarapandian S, Clemmer DE. Transfer of structural elements from compact to extended states in unsolvated ubiquitin. *J Am Chem Soc*. 2006;128(35):11713-11719.
8. Koeniger SL, Merenbloom SI, Clemmer DE. Evidence for many resolvable structures within conformation types of electrosprayed ubiquitin ions. *J Phys Chem*. 2006;110:7017-7021.
9. Merenbloom SI, Flick TG, Williams ER. How hot are your ions in TWAVE ion mobility spectrometry? *J Am Soc Mass Spectrom*. 2012; 23:553-562.
10. Shelimov KB, Clemmer DE, Hudgins RR, Jarrold MF. Protein structure in vacuo: Gas-phase conformations of BPTI and cytochrome c. *J Am Chem Soc*. 1997;119:2240-2248.
11. Uetrecht C, Rose RJ, van Duijn E, Lorenzen K, Heck AJR. Ion mobility mass spectrometry of proteins and protein assemblies. *Chem Soc Rev*. 2010;39(5):1633-1655.
12. Bush MF, Hall Z, Giles K, Hoyes J, Robinson CV, Ruotolo BT. Collision cross sections of proteins and their complexes: A calibration framework and database for gas-phase structural biology. *Anal Chem*. 2010;82(22):9557-9565.
13. Jurneczko E, Barran PE. How useful is ion mobility mass spectrometry for structural biology? The relationship between protein crystal structures and their collision cross sections in the gas phase. *Analyst*. 2011;136(1):20-28.
14. Wyttenbach T, Bowers MT. Structural stability from solution to the gas phase: Native solution structure of ubiquitin survives analysis in a solvent-free ion mobility–mass spectrometry environment. *J Phys Chem B*. 2011;115(42):12266-12275.
15. Chen S-H, Russell DH. How closely related are conformations of protein ions sampled by IM-MS to native solution structures? *J Am Soc Mass Spectrom*. 2015;26(9):1433-1443.
16. Takats Z, Wiseman JM, Gologan B, Cooks RG. Mass spectrometry sampling under ambient conditions with desorption electrospray ionization. *Science*. 2004;306(5695):471-473.
17. McEwen CN, McKay RG, Larsen BS. Analysis of solids, liquids, and biological tissues using solid probe introduction at atmospheric pressure on commercial LC/MS instruments. *Anal Chem*. 2005;77(23): 7826-7831.
18. Van Berkel GJ, Kertesz V, Koeplinger KA, Vavrek M, Kong ANT. Liquid microjunction surface sampling probe electrospray mass spectrometry for detection of drugs and metabolites in thin tissue sections. *J Mass Spectrom*. 2008;43(4):500-508.
19. Kertesz V, Van Berkel GJ. Scanning and surface alignment considerations in chemical imaging with desorption electrospray mass spectrometry. *Anal Chem*. 2008;80(4):1027-1032.
20. Jackson AU, Talaty N, Cooks RG, Van Berkel GJ. Salt tolerance of desorption electrospray ionization (DESI). *J Am Soc Mass Spectrom*. 2007;18(12):2218-2225.

21. Gao L, Li G, Cyriac J, Nie Z, Cooks RG. Imaging of surface charge and the mechanism of desorption electrospray ionization mass spectrometry. *J Phys Chem C*. 2010;114:5331-5337.
22. Wiseman JM, Ifa DR, Song Q, Cooks RG. Tissue imaging at atmospheric pressure using desorption electrospray ionization (DESI) mass spectrometry. *Angew Chem Int Ed*. 2006;45:7188-7192.
23. Eberlin LS, Liu X, Ferreira CR, Santagata S, Agar NYR, Cooks RG. Desorption electrospray ionization then MALDI mass spectrometry imaging of lipid and protein distributions in single tissue sections. *Anal Chem*. 2011;83(22):8366-8371.
24. Roach PJ, Laskin J, Laskin A. Nanospray desorption electrospray ionization: An ambient method for liquid-extraction surface sampling in mass spectrometry. *Analyst*. 2010;135(9):2233-2236.
25. Griffiths RL, Sisley EK, Lopez-Clavijo AF, Simmonds AL, Styles IB, Cooper HJ. Native mass spectrometry imaging of intact proteins and protein complexes in thin tissue sections. *Int J Mass Spectrom*. 2019; 437:23-29.
26. Breuker K, McLafferty FW. Stepwise evolution of protein native structure with electrospray into the gas phase, 10^{-12} to 10^{2} s. *Proc Natl Acad Sci*. 2008;105:18145-18152.
27. Trimpin S. Novel ionization processes for use in mass spectrometry: 'Squeezing' nonvolatile analyte ions from crystals and droplets. *Rapid Commun Mass Spectrom*. 2019;33(SI):96-120.
28. Peacock PM, Zhang WJ, Trimpin S. Advances in ionization for mass spectrometry. *Anal Chem*. 2017;89(1):372-388.
29. Trimpin S. "Magic" ionization mass spectrometry. *J Am Soc Mass Spectrom*. 2016;27(1):4-21.
30. Trimpin S, Inutan ED, Karki S, et al. Fundamental studies of new ionization technologies and insights from IMS-MS. *J Am Soc Mass Spectrom*. 2019;30(6):1133-1147.
31. Inutan ED, Trimpin S. Matrix assisted ionization vacuum, a new ionization method for biological materials analysis using mass spectrometry. *Mol Cell Proteomics*. 2013;12(3):792-796.
32. Trimpin S, Wang B, Inutan ED, et al. A mechanism for ionization of nonvolatile compounds in mass spectrometry: Considerations from MALDI and inlet ionization. *J Am Soc Mass Spectrom*. 2012;23: 1644-1660.
33. Trimpin S, Inutan ED, Herath TN, McEwen CN. Laserspray ionization – A new atmospheric pressure MALDI method for producing highly charged gas-phase ions of peptides and proteins directly from solid solutions. *Mol Cell Proteomics*. 2010;9(2):362-367.
34. Trimpin S, Herath TN, Inutan ED, et al. Field-free transmission geometry atmospheric pressure matrix-assisted laser desorption/ionization for rapid analysis of unadulterated tissue samples. *Rapid Commun Mass Spectrom*. 2009;23(18):3023-3027.
35. McEwen CN, Larsen BS. Fifty years of desorption ionization of nonvolatile compounds. *Int J Mass Spectrom*. 2015;377:515-531.
36. Inutan ED, Richards AL, Wager-Miller J, Mackie K, McEwen CN, Trimpin S. Laserspray ionization – a new method for protein analysis directly from tissue at atmospheric pressure with ultrahigh mass resolution and electron transfer dissociation. *Mol Cell Proteomics*. 2011;10:1-8.
37. McEwen CN, Pagnotti V, Inutan ED, Trimpin S. New paradigm in ionization: Multiply charged ion formation from a solid matrix without a laser or voltage. *Anal Chem*. 2010;82(22):9164-9168.
38. Richards AL, Lietz CB, Wager-Miller J, Mackie K, Trimpin S. Imaging mass spectrometry in transmission geometry. *Rapid Commun Mass Spectrom*. 2011;25(6):815-820.
39. Wang B, Dearring CL, Wager-Miller J, Mackie K, Trimpin S. Drug detection and quantification directly from tissue using novel ionization methods for mass spectrometry. *Eur J Mass Spectrom*. 2015;21(3):201-210.
40. Karki S, Meher AK, Inutan ED, et al. Development of a robotics platform for automated multi-ionization methods for mass spectrometry. *Rapid Commun Mass Spectrom*. 2019. https://doi.org/10.1002/rcm.8449
41. Lietz CB, Richards AL, Ren Y, Trimpin S. Inlet ionization: Protein analyses from the solid state without the use of a voltage or a laser producing up to 67 charges on the 66 kDa BSA protein. *Rapid Commun Mass Spectrom*. 2011;25(22):3453-3456.
42. Horan AJ, Apsokardu MJ, Johnston MV. Droplet assisted inlet ionization for online analysis of airborne nanoparticles. *Anal Chem*. 2017;89(2):1059-1062.
43. Trimpin S, Lee C, Weidner SM, et al. Unprecedented ionization processes in mass spectrometry provide missing link between ESI and MALDI. *ChemPhysChem*. 2018;19(5):581-589.
44. Pagnotti VS, Chakrabarty S, Harron AF, McEwen CN. Increasing the sensitivity of liquid introduction mass spectrometry by combining electrospray ionization and solvent assisted inlet ionization. *Anal Chem*. 2012;84(15):6828-6832.
45. Wang B, Trimpin S. High-throughput solvent assisted ionization *inlet* for use in mass spectrometry. *Anal Chem*. 2014;86(2):1000-1006.
46. Trimpin S, Lutomski CA, El-Baba TJ, et al. Magic matrices for ionization in mass spectrometry. *Int J Mass Spectrom*. 2015;377(SI): 532-545.
47. Marshall DD, Inutan ED, Wang B, et al. A broad-based study on hyphenating new ionization technologies with MS/MS for PTM's and tissue characterization. *Proteomics*. 2016;16(11-12):1695-1706.
48. Chubatyi ND, McEwen CN. Improving the sensitivity of matrix-assisted ionization (MAI) mass spectrometry using ammonium salts. *J Am Soc Mass Spectrom*. 2015;26(10):1649-1656.
49. Trimpin S, Inutan ED. Matrix assisted ionization in vacuum, a sensitive and widely applicable ionization method for mass spectrometry. *J Am Soc Mass Spectrom*. 2013;24(5):722-732.
50. Inutan ED, Trimpin S. Laserspray ionization (LSI) ion mobility spectrometry (IMS) mass spectrometry. *J Am Soc Mass Spectrom*. 2010;21(7):1260-1264.
51. Li J, Inutan ED, Wang B, et al. Matrix assisted ionization: New aromatic and non aromatic matrix compounds producing multiply charged lipid, peptide, and protein ions in the positive and negative mode observed directly from surfaces. *J Am Soc Mass Spectrom*. 2012;23(10):1625-1643.
52. Lu I-C, Pophristic M, Inutan ED, McKay RG, McEwen CN, Trimpin S. Simplifying the ion source for mass spectrometry. *Rapid Commun Mass Spectrom*. 2016;30(23):2568-2572.
53. Lu I-C, Elia EA, Zhang WJ, et al. Development of an easily adaptable, high sensitivity source for inlet ionization. *Anal Methods*. 2017;9: 4971-4978.
54. Konermann L, Douglas DJ. Unfolding of proteins monitored by electrospray ionization mass spectrometry: A comparison of positive and negative ion modes. *J Am Soc Mass Spectrom*. 1998;9:1248-1254.
55. Freitas MA, Hendrickson CL, Emmett MR, Marshall AG. Gas-phase bovine ubiquitin cation conformation resolved by gas-phase hydrogen/deuterium exchange rate and exten. *Int J Mass Spectrom*. 1999;185/186/187:565-575.
56. Purves RW, Barnett DA, Ells B, Guevremont R. Investigation of bovine ubiquitin conformers separated by high-field asymmetric waveform ion mobility spectrometry: Cross section measurements using energy-loss experiments with a triple quadrupole mass spectrometer. *J Am Soc Mass Spectrom*. 2000;11(8):738-745.
57. Purves RW, Barnett DA, Ells B, Guevremont R. Elongated conformers of charge states 111 to 115 of bovine ubiquitin studied using ESI-FAIMS-MS. *J Am Soc Mass Spectrom*. 2001;12:894-901.
58. Reid GE, Wu J, Chrisman PA, Wells JM, McLuckey SA. Charge-state-dependent sequence analysis of protonated ubiquitin ions via ion trap tandem mass spectrometry. *Anal Chem*. 2001;73(14):3274-3281.
59. Breuker K, Oh H, Horn DM, Cerda BA, McLafferty FW. Detailed unfolding and folding of gaseous ubiquitin ions characterized

by electron capture dissociation. *J Am Chem Soc*. 2002;124 (22):6407-6420.
60. Koeniger SL, Clemmer DE. Resolution and structural transitions of elongated states of ubiquitin. *J Am Soc Mass Spectrom*. 2007;18(2): 322-331.
61. Shvartsburg AA, Li F, Tang K, Smith RD. Distortion of ion structures by field asymmetric waveform ion mobility spectrometry. *Anal Chem*. 2007;79(4):1523-1528.
62. Flick TG, Cassou CA, Chang TM, Williams ER. Solution additives that desalt protein ions in native mass spectrometry. *Anal Chem*. 2012;84 (17):7511-7517.
63. Jhingree JR, Barran PE. Ion-ion interactions affect (re)folding dynamics of ubiquitin ions in the gas phase. Distinct folding intermediates formed via charge-reduction pathways. *ChemRxiv*. 2017Preprint. https://doi.org/10.26434/chemrxiv.5678872.v1
64. Inutan ED, Trimpin S. Laserspray ionization-ion mobility spectrometry –mass spectrometry: Baseline separation of isomeric amyloids without the use of solvents desorbed and ionized directly from a surface. *J Proteome Res*. 2010;9:6077-6681.
65. Pringle SD, Giles K, Wildgoose JL, et al. An investigation of the mobility separation of some peptide and protein ions using a new hybrid quadrupole/travelling wave IMS/oa-ToF instrument. *Int J Mass Spectrom*. 2007;261:1-2.
66. Trimpin S, Inutan ED. New ionization method for rapid analysis on API mass spectrometers requiring only vacuum and matrix assistance. *Anal Chem*. 2013;85(4):2005-2009.
67. Ewing MA, Glover MS, Clemmer DE. Hybrid ion mobility and mass spectrometry as a separation tool. *J Chromatogr A*. 2015;1439:3-25.
68. Trimpin S, Tan B, O'Dell DK, et al. Profiling of phospholipids and related lipid structures using multidimensional ion mobility spectrometry-mass spectrometry. *Int J Mass Spectrom*. 2009;287 (1–3):58-69.
69. Kelly RT, Tolmachev AV, Page JS, Tang K, Smith RD. The ion funnel: Theory, implementations, and applications. *Mass Spectrom Rev*. 2010; 29(2):294-312.
70. Kim T, Tang K, Udseth HR, Smith RD. A multicapillary inlet jet disruption electrodynamic ion funnel interface for improved sensitivity using atmospheric pressure ion sources. *Anal Chem*. 2001; 73(17):4162-4170.
71. Tang K, Aleksey V, Tolmachev AV, et al. Independent control of ion transmission in a jet disrupter dual-channel funnel electrospray ionization MS interface. *Anal Chem*. 2002;74(20):5431-5437.
72. Tang K, Page JS, Smith RD. Charge competition and the linear dynamic range of detection in electrospray ionization mass spectrometry. *J Am Soc Mass Spectrom*. 2004;15(10):1416-1423.
73. Kurulugama RT, Valentine SJ, Sowell RA, Clemmer DE. Development of a high-throughput IMS-IMS-MS approach for analyzing mixtures of biomolecules. *J Proteomics*. 2008;71(3):318-331.
74. McEwen CN, Larsen BS, Trimpin S. Laserspray ionization on a commercial atmospheric pressure-MALDI mass spectrometer ion source: Selecting singly or multiply charged ions. *Anal Chem*. 2010;82 (12):4998-5001.
75. McEwen CN, Simonsick WJ, Larsen BS, Ute K, Hatad K. The fundamentals of applying electrospray ionization mass spectrometry to low mass poly (methyl methacrylate) polymers. *J Am Soc Mass Spectrom*. 1995;6(10):906-911.
76. Wyttenbach T, Kemper PR, Bowers MT. Design of a new electrospray ion mobility mass spectrometer. *Int J Mass Spectrom*. 2001;212: 13-23.
77. Inutan ED, Wang B, Trimpin S. Commercial intermediate pressure MALDI ion mobility spectrometry mass spectrometer capable of producing highly charged laserspray ionization ions. *Anal Chem*. 2011; 83(3):678-684.
78. Trimpin S, Lu I-C, Rauschenbach S, et al. Spontaneous charge separation and sublimation processes are ubiquitous in nature and in ionization processes in mass spectrometry. *J Am Soc Mass Spectrom*. 2018;29(2):304-315.
79. Fenner MA, McEwen CN. Survival yield comparison between ESI and SAII: Mechanistic implications. *Int J Mass Spectrom*. 2015;378: 107-112.
80. El-Baba TJ, Woodall DW, Raab SA, et al. Melting proteins: Evidence for multiple stable structures upon thermal denaturation of native ubiquitin from ion mobility spectrometry-mass spectrometry measurements. *J Am Soc Mass Spectrom*. 2017;139:6306-6309.
81. Wang B, Akhmetova E, Trimpin S, Wilkins CL. Matrix-assisted ionization vacuum for high-resolution Fourier transform ion cyclotron resonance mass spectrometers. *Anal Chem*. 2014;86(14): 6792-6796.
82. Trimpin S, Ren Y, Wang B, et al. Extending the laserspray ionization concept to produce highly charged ions at high vacuum on a time-of-flight mass analyzer. *Anal Chem*. 2011;83(14):5469-5475.

SUPPORTING INFORMATION

Additional supporting information may be found online in the Supporting Information section at the end of this article.

How to cite this article: Inutan ED, Jarois DR, Lietz CB, et al. Comparison of gaseous ubiquitin ion structures obtained from a solid and solution matrix using ion mobility spectrometry/ mass spectrometry. *Rapid Commun Mass Spectrom*. 2021;35 (S1):e8793. https://doi.org/10.1002/rcm.8793